QUANTIFYING TRACK CONDITION BASED ON SOIL PROPERTIES

Jinse Schoorl

Cover picture: Pixabay, 2018

Jinse Schoorl
4910605

Supervising committee
V.L. Markine
A.A. Nunez Vicencio
K. El Laham

Bachelor Thesis
Civil Engineering and
Geosciences

Delft University of Technology

14-06-2021

Preface

This is the thesis ‘Quantifying track condition based on soil properties’. It is a research into the quantification of the influence of soil on the condition of railway tracks. This thesis has been written as part of the Civil Engineering Bachelor of the faculty Civil Engineering and Geosciences at the Delft University of Technology.

Readers are referred to chapters 3 and 4, if they are interested in the theoretical background of the research and the development of the assessment model. If readers are interested in the analysis of a trajectory and the evaluation of the results, they are advised to consult chapters 5 and 6.

I want to express my gratitude towards the three members of the supervising committee, Valeri Markine, Alfredo Nunez Vicencio and Karim El Laham, for their assistance and helpful feedback during the execution of this research.

Jinse Schoorl,

IJmuiden, June 14 2021

Summary

Soil is an important part of a railway track structure. It provides the foundation for the structure and distributes the imposed loads. Consequently, soil has an influence on the condition of a track structure and a low quality soil can ultimately cause failure of the track structure. To be able to include the condition of a soil in the assessment on track quality, the following research question is posed: "*What is the quantitative influence of soil on the track condition for the railway tracks between Utrecht and Den Bosch?"*

To be able to answer the research question, first the influence of soil on track condition is distinguished. The most important failure types, progressive shear failure and excessive plastic deformation, are best characterised by the strength of the soil and the deformation of the tracks respectively. For these characteristics a method is developed, which assesses the track condition. For strength a bearing capacity approach is used and for deformations a beam-on-an-elastic-foundation model is used. The process of the method is illustrated by executing it for a specific trajectory, being the Utrecht-Den Bosch line in the Netherlands. To take into account the variability of different soils, the soil type and some specific soil parameters derived from Cone Penetration Tests are determined and applied in the calculations for the assessment.

From the results can be concluded that for the Utrecht-Den Bosch line, the track quality considering passenger trains will either deteriorate limitedly or not at all. This is the case for quality related to both strength and deformation. For cargo trains, the quality related to deformation is such that limited deterioration can be expected. For strength, however, a large number of sections has a condition varying between the failure level and the desired level, which means that significant deterioration is possible, though, there are sections with higher quality as well.

Table of contents

1. Introduction

Rail infrastructure is an essential part of the railway system. The infrastructure is a critical component for operating a railway system. Since the infrastructure itself is highly important, the condition of it is as well. To maintain the quality of the infrastructure, maintenance is performed frequently. Important is to know when to perform the maintenance. If maintenance is not performed at the right instant, this could result in unnecessary costs and operational problems. A prediction of the track condition is hence critical for the operation of a railway network.

Soil is an essential part of a railway track structure. It distributes the load induced by the tracks and trains. If a soil is not able to successfully distribute the load and no actions are taken, this could damage the tracks and eventually result in failure of a track section, giving rise to a large impact on the railway system. Consequently, the characteristics of a soil should be included in the prediction of the track condition.

Even though soil is an essential part of a track structure, its influence on a track structure is not recognized easily. The performance of a soil depends on many parameters, making it difficult to evaluate the condition. Some parameters require laboratory testing as well. To be able to predict the track condition of a trajectory, the objective is to develop a method to predict the track condition using available data.

The research question following from this problem statement is:

What is the quantitative influence of soil on the track condition for the railway tracks between Utrecht and Den Bosch?

The research question will be answered using the following sub-questions:

- How is track condition influenced by underlying soil?
- How can track condition be quantified?
- Which types of soils are present under the railway tracks between Utrecht and Den Bosch?
- What is the track condition for the trajectory Utrecht-Den Bosch?

To be able to predict track condition based on the soil that supports the tracks and apply maintenance adequately and efficiently, firstly the behaviour of the soil needs to be understood. Based on this understanding, a method to predict the condition of the soil and track will be developed. The method can be applied on all track sections, yet in this report the track condition will be evaluated for the railway track section between Utrecht and Den Bosch in the Netherlands.

Chapter 2 elaborates on the methodology pursued to answer the research questions. Chapter 3 describes the influence soil has on a track structure. The quantification of the influence is addressed in chapter 4. In chapter 5 the soil parameters for the trajectory are classified, which are used in chapter 6 for the evaluation of the track condition. Finally, chapters 7 and 8 will discuss the conclusion and the discussion on the research.

2. Methodology

The first part of the research concerns the investigation of the influence of soil on track condition. Literature is consulted to develop an understanding in the influence a soil has on the condition of railway tracks and what the most important aspects are to consider when assessing track condition. The literature that is used comprises published research papers and books on the subject.

Based on the understanding of the influence, a method is developed, which quantifies the influence. For the two main characteristics concerning soil behaviour in railway tracks, existing literature is referenced to find formulas and relations that quantify the influence of soil, using specific soil parameters that can be derived from existing data. Besides formulas, a model is used for the quantification of the deformations in the rail. This is the Winkler model, which is a simplified approach to determine deformations in a track structure.

The next part is to retrieve values for the parameters to perform calculations. The values have been retrieved for the track section between Utrecht and Den Bosch. The trajectory is presented as sections of 200 m, all with specified coordinates. The values for the parameters have been determined exclusively for this set of coordinates. The data available to determine the values are soil classifications and Cone Penetration Tests (CPT). With regard to the CPT-tests, the values from the tests are averaged over the expected layer height of the top soil layer. Missing values are approximated with Inversed Distance Weighted interpolation.

Finally, by using the found equations and relations and implementing the acquired values for the parameters, the track condition is evaluated for the track section between Utrecht and Den Bosch. This enables the assessment on the condition of the track, related to the underlying soil.

3. Analysis of soil influence on track condition

Soil is an integral part of a railway track structure. Figure 1 shows a schematisation of a conventional ballasted track structure. A track structure is designed as such, that it disperses the large load induced by the train on the rails to a smaller, evenly spread load acting on the soil layer. The rail is the top part of the structure and it is attached to the sleepers. Sleepers are supported by ballast and sub-ballast layers. The lowest layer of the structure concerns the soil and it hence provides the foundation for all the parts that form the track structure. The soil in a track structure is often referred to as either subsoil or subgrade.

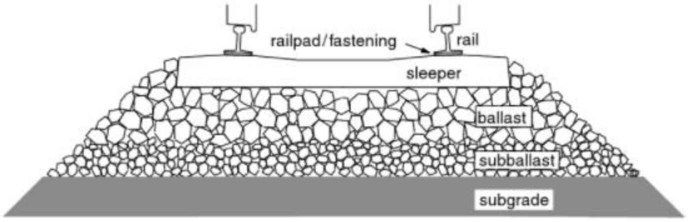

Figure 1 Schematisation of a conventional ballasted track structure (Taylor & Francis Group, LLC, 2006)

As the subsoil is the foundation of the track structure, problems related to the subsoil can cause failure of the complete track structure. Various types of subgrade problems can occur. These subgrade problems are caused by three different aspects: repeated traffic loading, weight of the train and the track structure, and environmental factors (Li & Selig, 1995). The main types of subgrade problems are problems related to repeated traffic loading. These subgrade problems are progressive shear failure and excessive plastic deformation (Li & Selig, 1998). Occasionally, attrition with mud pumping is listed as a third major problem. This problem, however, mainly concerns the ballast and sub-ballast layers rather than the subsoil. Therefore, it is not included in this research. Even though a number of other problems exists, solely the two problems mentioned will be discussed, as they are the most important problems.

Progressive shear failure occurs at the surface of the subsoil and is the result of repeated overstressing (Li & Selig, 1995, 1998). Because of the overstressing, the subsoil remoulds and it squeezes outward and upward, following the path of the least resistance. Figure 2 shows the process of progressive shear failure. The result is a larger ballast layer height under the tracks and the subsoil reaching the surface next to the tracks. This type of failure occurs mainly on fine-grained soils, clays for instance.

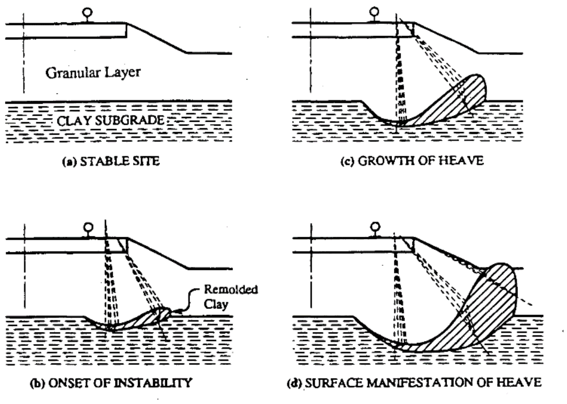

Figure 2 Process of progressive shear failure in a track structure (Li & Selig, 1995)

Excessive plastic deformation is, similar to progressive shear failure, the result of repeated loading (Li & Selig, 1995, 1998). Subgrade layer deformations are caused by the vertical component of the progressive shear deformation and the progressive compaction and consolidation of subgrade soils. As a result of that, ballast pockets are formed, as show in Figure 3. These ballast pockets make that the tracks lower. As the degree of excessive plastic deformation generally differs along the longitudinal section of tracks, the track geometry is likely to deform inconsistently. The longitudinal section in Figure 3 shows the inconsistent deformations that can occur. Excessive plastic deformation occurs mainly on fine-grained soils.

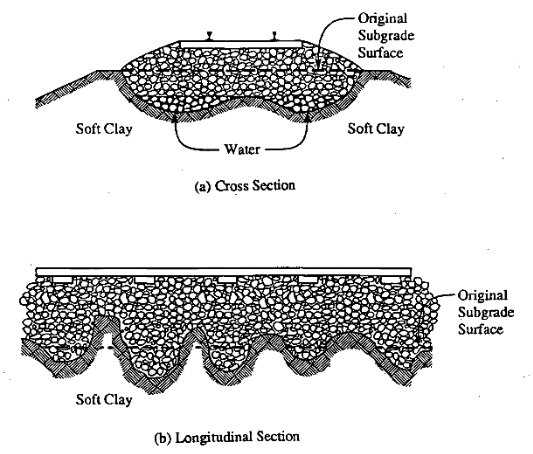

Figure 3 Illustration of excessive plastic deformation in a track structure (Li & Selig, 1995)

4. Quantification of track condition

Soil performance and quality is described by two characteristics: strength and deformation (McHenry & Rose, 2012). These characteristics closely relate to the aforementioned major problems for subsoils: progressive shear failure is dependent on the strength, more specifically the shear strength, of a soil, while excessive plastic deformation relates to deformations of the subsoil. Thus, a different method for each characteristic can be developed to determine the track quality, using soil properties related to these characteristics. In this chapter the process to determine the track quality will be described, which will be used for calculations in chapter 6.

4.1 Strength

The track condition related to strength can be described by the bearing capacity of the soil (McHenry & Rose, 2012). The bearing capacity is described as the maximum stress a foundation can withstand before it fails. Failure of a soil on bearing capacity is the heave of a part of the soil, like the heave that occurs with progressive shear failure. The quality of the soil related to bearing capacity is often given by the bearing capacity factor of safety (BCF), which is defined as the ratio between the bearing capacity of the soil and the actual stress in the soil. If the BCF is larger than 1.0, the soil will not fail instantly. Furthermore, a value close to 1 means that, even though the soil will not fail, deterioration of the track can still occur, given the characteristics of progressive shear failure as described in chapter 3. To take into account errors during the determination of the BCF and to maintain a margin to the failure point, generally a higher BCF is required. For the railway application the value is desirably between 2.0 and 2.5 (Sattler et al., 1989). A soil with a BCF in this range or higher can be expected not to deteriorate.

The equation to determine the bearing capacity can be used for all soil types and is the following (Sattler et al., 1989; Verruijt, 2010):

$$q_u = c' N_c + 0.5\gamma' B N_\gamma + q_o N_q \tag{1}$$

where

q_u	[kPa]	= bearing capacity;
N_c, N_γ, N_q	[-]	= bearing capacity factors;
c'	[kPa]	= subsoil cohesion;
γ'	[kN/m^3]	= effective volumetric weight of the subsoil;
B	[m]	= footing width;
q_o	[kPa]	= surcharge loading

The parameter *c'* and the effective volumetric weight γ' are dependent on the subsoil type and are input for the calculations. The apostrophes indicate that the bearing capacity analysis will be a drained analysis. A drained analysis means that effective stresses will be used. As the water in the soil has had time to drain, the soil skeleton fully carries the load and effective stresses are to be used. The magnitude of effective stresses depend on the ground water table. For a soil below the ground water table, a saturated soil, the total stress has to be reduced by the pore pressure of the water, which is 10 kN/m^3. For calculating bearing capacity, dry soil conditions can be assumed if the distance from the ground water table to the foundation level is larger than 1.5*B*, otherwise saturated soil conditions should be assumed (Hicks, presentation slides, March 5, 2020).

For the assessment of the bearing capacity, a cross-section perpendicular to the tracks is investigated, as failures in the perpendicular direction are more critical (Sattler et al., 1989). In the perpendicular cross-section, two types of failure are possible: the failure of the complete track system and the failure of a heavily stressed portion of the track system. The last failure type is the most significant and will hence be evaluated. The footing width *B* corresponding to this failure type is one third of the sleeper length. The conventional sleeper length in the Netherlands is 260 cm (COB, 1997). Consequently, the footing width *B* becomes 87 cm.

The surcharge loading q_o is the load applied on the subgrade next to the area on which the force acts. The foundation level considered is the surface of the subsoil. Next to the tracks, generally no additional layers are present on top of the subsoil, assuming the cross-section perpendicular to the tracks. The surcharge loading q_o is therefore equal to 0.

The bearing capacity factors in equation (1) are to be computed using the following equations (Verruijt, 2010):

$$N_q = e^{(\pi \tan(\phi'))} \left(\frac{1+\sin(\phi')}{1-\sin(\phi')} \right) \tag{2}$$

$$N_c = (N_q - 1)\cot(\phi') \tag{3}$$

$$N_\gamma = 2(N_q - 1)\tan(\phi') \tag{4}$$

where

ϕ' [deg] = soil friction angle

The parameter φ', similar to c', is dependent on the subsoil type and is input for the calculations.
To be able to calculate the BCF, aside from the bearing capacity itself, the actual stress at the subsoil surface needs to be determined. To determine the actual stress, a pyramid model will be used. This model describes the stress dispersion through the ballast layers. Figure 4 shows a schematisation of the model.

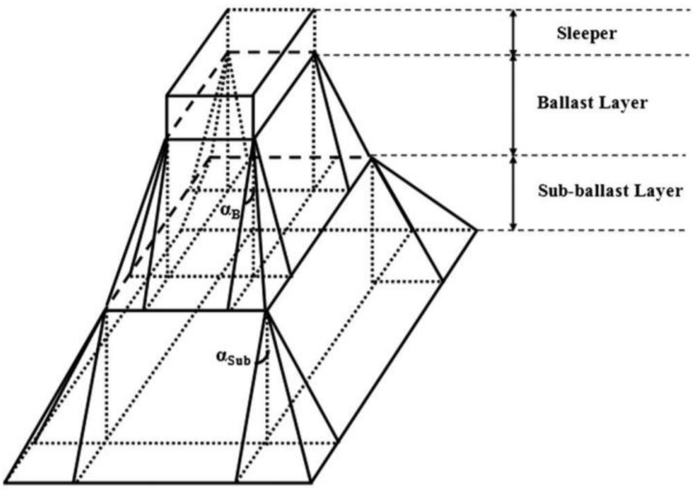

Figure 4 Schematisation of the stress distribution model (Mosayebi et al., 2020)

It is assumed that a single wheel load is spread over one third of the sleeper length. The stresses are then dispersed from the sleeper through the ballast and sub-ballast layer by the angles α_B and α_{sub} respectively. With these angles and the thicknesses of the ballast and sub-ballast layer, the total area in the perpendicular direction over which the force will be spread can be determined. For α_B and α_{sub} a value of 35° will be used (Mosayebi et al., 2016, 2020). For the ballast and sub-ballast layer thickness, conventional values will be used, which are respectively 30 cm and 10 cm (Esveld, 2001). This amounts to an additional width, next to one third of the sleeper length, of 28 cm at each side. The total length over which a single wheel load is spread is hence 143 cm.

In the direction parallel to the tracks, the same approach will be used. Considering a regular sleeper width of 30 cm and with the additional 28 cm at both sides, the spread length is 86 cm. As the load spread patterns coming from the sleepers do not overlap, overlapping has not to be accounted for. The total area over which the load is spread is thus 1.23 m^2.

Besides the area over which the load acts, the load itself needs to be determined as well. Passenger trains are logically operating on the trajectory. Besides passenger trains, several tracks in the Netherlands, including the trajectory Utrecht-Den Bosch, are part or will be part of cargo train corridors (Drenth, 2019). Consequently, two different train types will be considered: passenger trains and cargo trains.

The axle load of a passenger train with engine, a train that operates on the trajectory, is 170 kN (Railplaza.nl, 2021). The maximum velocity of these trains for the trajectory Utrecht-Den Bosch is 130 km/h (ProRail, 2020). On cargo corridors, the weight allowed to be exerted on an axle is 22.5 tons. The axle load will hence be 221 kN. The maximum velocity for cargo trains is 100 km/h.

As trains are not stationary, they cause dynamic effects as well. To include the dynamic effects into the calculation, the applied dynamic load P_d will be used. P_d is calculated using the following formula (Wang et al., 2020):

$$P_d = \varphi P_s \tag{5}$$

where

P_d [kN] = applied dynamic load;
ϕ [-] = dynamic amplification factor;
P_s [kN] = applied static load

For φ the following formula will be used (Sun et al., 2016):

$$\varphi = e^{0.003V} \tag{6}$$

where

V [km/h] = velocity of the train

This formula better approaches the true value for the dynamic amplification factor at lower speeds than other methods. For P_s, the axle loads will be divided by 2 to come to a single wheel load. Given the provided values, φ is 1.48 and P_d 126 kN for a passenger train. For a cargo train φ is 1.35 and P_d 149 kN. With the area of 1.23 m^2 over which the load spreads, the exerted pressure by a single wheel dynamic load becomes 102 kPa for passenger trains and 121 kPa for cargo trains.

To account for the weight of the ballast and sub-ballast layer, these layers will be included in the applied pressure. The unit weight of the ballast and sub-ballast layers are respectively 17.3 kN/m^3 and 18.8 kN/m^3 (Li & Selig, 1994, 1998). Multiplying with the height of each layer, the additional pressure exerted by the ballast and sub-ballast amounts to a total of 7 kPa. The additional weight of the rails and sleepers is negligible. The total applied pressures are respectively 109 kPa and 128 kPa for passenger trains and cargo trains.

4.2 Deformation

The condition of tracks considering deformations can be described by deformations of the rails. The vertical deformation of a rail is an indicator for the quality of the track. As deformations can be both elastic and plastic, a method is required to relate elastic deformation to plastic deformation. Figure 5 shows a method, which distinguishes several domains that relate elastic deformation to long-term behaviour.

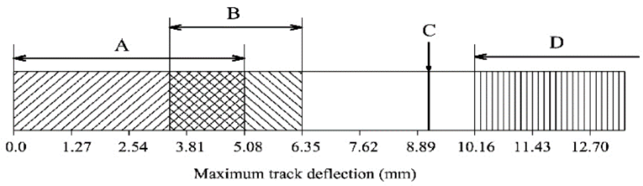

Figure 5 Domains for the classification of deformations (Sadeghi & Barati, 2010)

Domain A is an indication for a track structure that deforms even less than allowed and is therefore largely sufficient. Domain B is the desired domain and point C is a limit for the deflection of light-weight tracks. The final domain, domain D, displays the deformations for which tracks deform more than allowed and hence indicates that tracks will deteriorate quickly (Sadeghi & Barati, 2010). Track sections can thus be classified on both elastic and plastic deformation using Figure 5.

In order to classify the track sections, the expected deformations have to determined. In order to do so, the track-soil system will be modelled as a beam on an elastic foundation (BOEF) or, more specifically, as a Winkler model. The Winkler model is a simplified model of the track system, which relates well to the reality (van Belkom, 2020). Figure 6 shows a simple form of the Winkler model.

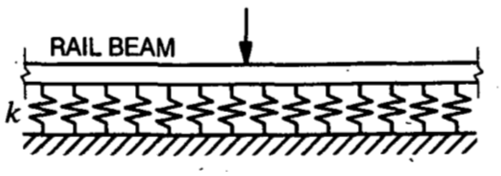

Figure 6 Structure of the Winkler model (Bathurst, 1994)

The model describes the vertical deflection caused by a point load P_d, which is calculated using equations (5) and (6). The wheel loads as listed in section 4.1 will be used.
For the conventional Winkler model, the differential equation that needs to be solved is the following (Arthur & Richard, 2002; Li & Selig, 1994):

$$EI\frac{d^4w}{dx^4} = -kw \tag{7}$$

where

E [MPa] = Young's modulus of the rail;
I [mm^4] = Moment of inertia of the rail;
w [mm] = Vertical deflection of the rail;
x [mm] = Horizontal position along the rail;
k [MPa] = Combined spring coefficient

The value of E for rails in the Netherlands is 210 x 10^3 MPa and the value for I is 23.46 x 10^6 mm^4 (COB, 1997). The spring coefficient k is the spring coefficient of the complete track structure, for a track structure consists of different parts with different stiffnesses. The stiffnesses of the different parts can be combined using the following relation (Bathurst, 1994; Prakoso, 2016):

$$\frac{1}{k_{tot}} = \frac{1}{k_{rail-pad}} + \frac{1}{k_{fastener}} + \frac{1}{k_{ballast}} + \frac{1}{k_{sub-ballast}} + \frac{1}{k_{subsoil}} \tag{8}$$

where

k_i [N/mm^2] = spring coefficient of element i

The value for $k_{ballast}$ is 150 N/mm^2 and, considering a regular sleeper distance of 0.7 m, the values for $k_{rail-pad}$ and $k_{fastener}$ are 2029 N/mm^2 and 21 N/mm^2 (COB, 1997). For $k_{sub-ballast}$ a value of 80 N/mm^2 is used (Shahu et al., 1999). Sleepers are assumed not to deform, for they are supported from the sides and from below (Prakoso, 2016). Hence, they are not included in the stiffness modulus. The value for $k_{subsoil}$ is dependent on the soil type and is input for the calculations.

5. Analysis of soil composition trajectory Utrecht-Den Bosch

In order to illustrate the process, the track condition for the trajectory Utrecht-Den Bosch will be evaluated. The values that are input for the calculations, have to be determined first. In this chapter, the trajectory will be briefly described and the soil composition under the trajectory will be analysed, followed by the evaluation of the parameters, which can be done based on the soil classification.

5.1 Description of the trajectory

The trajectory for which the track condition will be evaluated is the trajectory Utrecht-Den Bosch in the Netherlands. This trajectory is a predominantly two-track trajectory. Figure 7 shows the location of the trajectory. The trajectory will be analysed by dividing it into sections of at most 200 m in length.

The trajectory crosses several rivers and canals. This is done by bridges crossing over these waterways. As the tracks at these bridges are not directly supported by soil, the condition of the track and soil under these bridges cannot be determined with the approach described in this report. These sections will therefore be emitted from the analysis. Furthermore, the trajectory crosses several dikes. As dikes have a complex composition with different soil types, dikes will be emitted from the analysis as well.

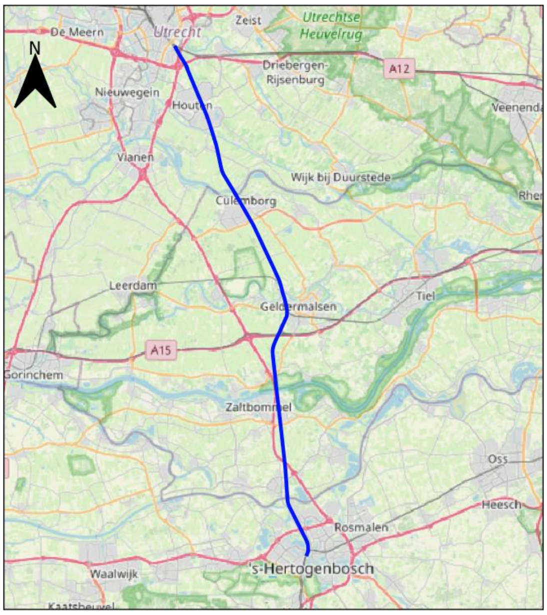

Figure 7 Map of the trajectory Utrecht-Den Bosch

5.2 Soil type classification

Soil types are classified using a map of the soil composition in the Netherlands. The map that is used is created by the TU Delft (TU Delft Library, n.d.). The soil types as indicated in the map will be retrieved for every section along the trajectory Utrecht-Den Bosch.

The soil types in the soil map are classified according to the descriptions listed by Ten Cate et al. (1995). These soil type classifications will be simplified to a soil type and an admixture. The soil types and admixtures used are listed in Appendix A. Several soils are classified as coarse sand, a soil with both clay and sand contents. Table 1 shows the difference between sand, coarse sand, in Dutch referred to as zavel, and clay. Following this division, light zavel is characterised as clayey sand and both zavel and heavy zavel as sandy clay. For some locations, the soil type is not provided in the map, as the location is classified as an urban area, for instance. Models about the soil composition created by TNO GDN are used to acquire data for these locations (TNO GDN, n.d.).

Table 1 Distinction between sand, coarse sand and clay (Stichting voor Bodemkartering, 1991)

% lutum	naam	samenvattende naam	
0 – 5	kleiarm zand		zand[1]
5 – 8	kleiig zand		
8 – 12	zeer lichte zavel	lichte zavel	zavel
12 – 17,5	matig lichte zavel		
17,5 – 25	zware zavel		
25 – 35	lichte klei		klei
35 – 50	matig zware klei	zware klei	
50 – 100	zeer zware klei		

[1] Tevens meer dan 50% zandfractie (50–2000 µm).

From the analysis can be concluded that a large majority of the trajectory is based on a clay layer, either regular clay or sandy clay. A small part of the trajectory is based on sand, predominantly clean sand, and another small part is based on a sandy loam layer.

5.3 Evaluation of parameters

Four parameters need to be evaluated in order to assess the track condition. These are the angle of friction *φ'*, cohesion *c'*, effective volumetric weight *γ'* and the subsoil modulus $k_{subsoil}$. Next to the soil type, two soil properties need to be determined from CPT-tests to be able to determine these four parameters. These soil properties are the cone resistance q_c and the sleeve friction f_s.

The value of a soil property will be estimated based on the expected height of the top layer and the average value of the property along that part of the CPT-plot. The CPT-tests that will be used are provided by TNO GDN (n.d.). Since CPT-tests have not been done for every section, predictions and estimates regarding non-tested sections need to be made. Firstly, for each section itself, a single value will be assumed to be governing along the complete section. If a CPT-test is done in a section, the found value for a property is used. If no test is done in a section, the value will be interpolated. The interpolation method that is used is Inverse Distance Weighted interpolation or, in short, IDW. This method is simple to execute and has proved to be an accurate method (Rahman, 2018). The formula is the following:

$$x_0 = \frac{\sum_{i=1}^{n} x_i \frac{1}{d_i^m}}{\sum_{i=1}^{n} \frac{1}{d_i^m}} \tag{9}$$

where

x_0 [MPa] = Estimated value for parameter x
x_i [MPa] = Observed value for parameter x
d_i [m] = Distance between location of estimation and location of measurement
m [-] = Power parameter

A value of 2 will be used for the parameter *m*. IDW-interpolation will be done using test data from points on the train line, as a large number of testing locations is on or very near to the train line. The closest point on either side of the section, for the trajectory Utrecht-Den Bosch one point to the north and one point to the south, will be used. If the distance of a point, which is not located on or very near the train line, is closer to the section than either one of the two points on the line, this point will be included in the interpolation as well. If the distance of a point is larger, the contribution of this point will be small, since the value of *m* is larger than 1. The distances from measurement points to points of estimation will be estimated. Multiple testing points that describe the same soil, i.e. are at the same location, will be included as one single point. Interpolation will not be done between soils with a different range of q_c-value, such as clay or loam in comparison with sand. As the properties of these soil types are highly different, interpolation will not yield accurate values. If no testing data is available for a certain soil type, the value of the closest soil with the same soil type will be used.

With the soil properties known, the four parameters can be evaluated. The angle of friction φ' can be determined with the cone resistance and the pore pressures. The following equations will be used to determine the angle of friction for sand (Rocscience Inc., 2016 & Saftner, 2018):

$$\varphi' = 17.6 + 11 \log Q_{tn} \tag{10}$$

$$Q_{tn} = \left(\frac{q_c - \sigma_{v0}}{P_a} \right) \left(\frac{P_a}{\sigma'_{v0}} \right)^n \tag{11}$$

$$n = 0.381 I_c + 0.05(\sigma'_{v0} / P_a) - 0.15 \tag{12}$$

$$I_c = ([3.47 - \log((q_c - \sigma_{v0}) / \sigma'_{v0})]^2 + [\log(f_s / (q_c - \sigma_{v0})) + 1.22]^2)^{0.5} \tag{13}$$

where

q_c [MPa] = cone resistance
P_a [MPa] = atmospheric pressure
n [-] = stress exponent
σ_{v0} [MPa] = total overburden stress
σ'_{v0} [MPa] = effective overburden stress
f_s [MPa] = sleeve friction

For P_a a value of 0.1013 MPa is used (ACS Distance Education, 2021). Since the foundation level is the ground level, the overburden stress is equal to the pressure exerted by the ballast and sub-ballast layer, which is 7 kPa. In other literature, the value of q_c is corrected for the shape of the testing cone. However, this correction is negligible and therefore simply q_c will be used. If insufficient data can be found to perform the calculations, lower bound values of φ' will be used. These are listed in Appendix A. For non-sandy soils tabulated values will be used to estimate the angle of friction. Based on the soil type and admixture the friction angle can be determined. The values are listed in Appendix A.

For c' and γ specific values for each soil type exist. Average values have been used for the volumetric weights. The table with the values is listed in Appendix A. The cohesion of fine-grained soils cannot be specified further than a range of possible values.

To determine whether the dry volumetric weight γ_d or the saturated volumetric weight γ_{sat} should be used, the ground water level is required. Dry soil conditions may be assumed, if the ground water table is at a minimum distance of 1.5*B*, 131 cm, from the foundation level, which is the ground level. If the distance is smaller than 1.5*B*, saturated soil conditions have to be assumed. Using ground water table data provided by TNO GDN (n.d.), for each section is determined if the ground water table is closer than 1.5*B* to the ground level during the time period of the available data. The maximum values of the ground water table are considered, as saturated conditions are governing for the bearing capacity. Consequently, saturated conditions are used if the available data do not show a consistent pattern.

The last parameter to be evaluated is the subsoil modulus $k_{subsoil}$. With the cone resistance, the sleeve friction and equation (13), $k_{subsoil}$ can be determined. The following equation is used (Rocscience Inc., 2016):

$$k_{subsoil} = 0.015(10^{0.55 I_c + 1.68})(q_c - \sigma_{v0}) \tag{14}$$

6. Evaluation of track condition for trajectory Utrecht-Den Bosch

As all the required formulas and parameters are presented, the evaluation of the track quality can be performed. The condition regarding the two characteristics, strength and deformation, will be calculated and assessed for both passenger trains and cargo trains. In this chapter the results will be presented graphically. For the procedure that has been followed to come to these results, Appendix B can be consulted. A reflection on the result will be given as well.

6.1 Strength assessment

The point of assessment of the strength is the bearing capacity factor of safety (BCF). A BCF smaller than 1 indicates that bearing capacity failure will occur. As mentioned in section 4.1, a value of 2 to 2.5 is desired for railway engineering practices.

Based on the values and equations determined in previous chapters, the BCF's have been determined. The results are presented in maps. Figure 8 and Figure 9 show the trajectory where each section is marked with a small line segment. Figure 8 is the figure for passenger trains and Figure 9 the figure for cargo trains. A red line segment is a section which includes BCF-values up to 1.1, a ten percent margin on the failure point. These sections are thus close to failure according to the computations. Yellow line segments are sections with a value between 1.1 and 2. These are section that are not close to failure, yet are not of desired quality either. Green line segments are sections with a BCF larger than 2, i.e. sections that are of desired quality. Black line segments are sections that are not assessed, e.g. bridges.

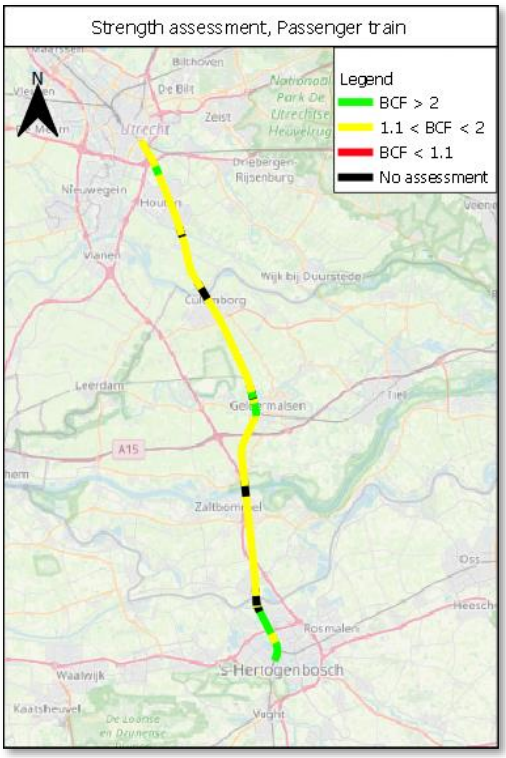

Figure 8 Map of track condition related to strength for passenger trains

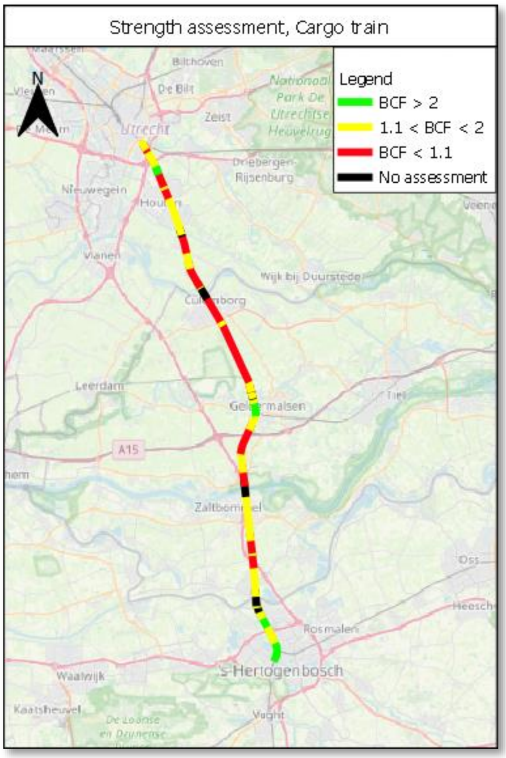

Figure 9 Map of track condition related to strength for cargo trains

Since an exact value for the cohesion of cohesive soils cannot be determined, a range of possible values for the BCF exists. Figure 8 and Figure 9 are based on the lower bound value of the range of possible values, as this yields the lowest BCF. The value can in reality be the upper bound as well. From the calculations can be seen that, for the given cohesion range, the BCF using upper bound values is approximately a factor 2 larger than the BCF using lower bound values. This means that for upper bound cohesion values red line segments are in the range of the desired quality by a very small margin and yellow line segments are of the desired quality.

6.2 Deformation assessment

The deformations will be assessed with Figure 5. Similarly to Figure 8 and Figure 9, Figure 10 and Figure 11 have been composed. Figure 10 is based on passenger train loading and Figure 11 on cargo train loading. In this case, red line segments are segments with a deformation *w* larger than 10.16 mm, the limit of domain D from Figure 5. Green segments are segments with a deformation smaller than 6.35 mm, the upper bound of domain B. Yellow segments have deformations in between the two limit values and black segments are not assessed. If a segment is green, that thus means that the section will maintain a good condition over a long-term period. On the contrary, a red segment will deteriorate quickly over time. Yellow segments will be a combination of the two: they will likely maintain a sufficient quality, yet undergo some deterioration as well. It should be noted that the transition between two differently coloured segments is not necessarily as sudden as the figures show, except for transition with black segments, as in several cases, adjacent segment have deformations that differ by only a small amount.

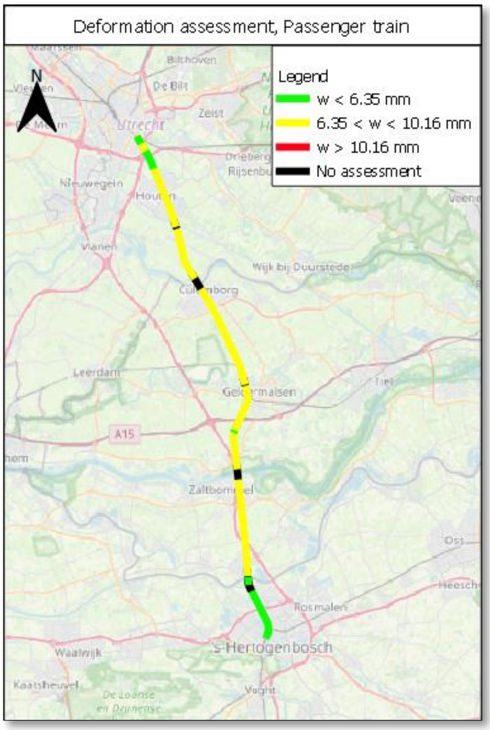

Figure 10 Map of track condition related to deformation for passenger trains

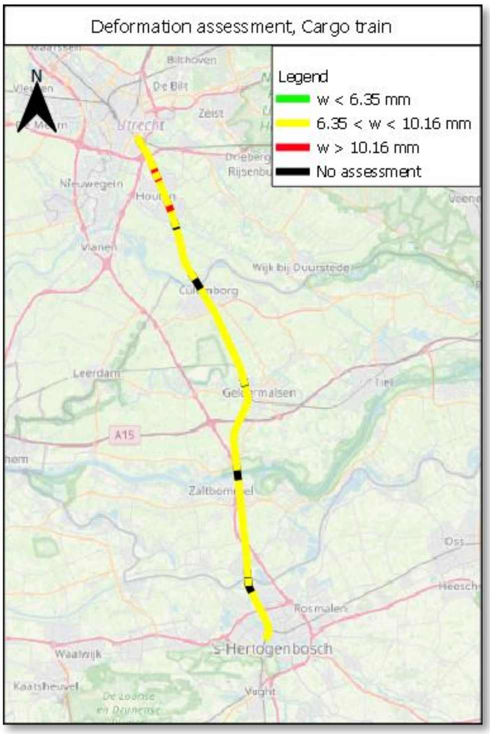

Figure 11 Map of track condition related to deformation for cargo trains

6.3 Reflection on the results

It is important to have consistency in the results and to relate the results to the real-life behaviour of the soil. The results are consistent considering the strength. The results show that a sand has a high strength and will likely suffice as a foundation. For clays, the strength is generally sufficient to prevent failure, yet significantly less than for sands, which follows the expectations. The method shows furthermore that peat soils have insufficient strength for a railway foundation. Since peat soils, in general, are soils with low bearing capacity, this follows the expectations (Ibrahim et al., 2014).

In terms of the relation with real-life behaviour, the calculated bearing capacities match with the typical range of bearing capacities that can exist, according to Nuevvo (2021a). The bearing capacity of clay, for instance, varies between 130 kPa to, in specific cases, 400 kPa, which is in line with the provided range. For sands, however, the model tends to predict a bearing capacity larger than the provided values. Yet, since no upper bounds are provided, the predicted values are not incorrect. The higher bearing capacity is possibly explained by the relatively large angle of friction that can be found in shallow sand layers (Ramadan et al., 2015).

With regard to the strength assessment for fine-grained soils, the two parameters with the most significant influence on the outcome are the friction angle and the cohesion. These parameters are determined based on specifically the soil type and therefore have some variability in their values. As no specific cohesion value can be determined, the variability of cohesion is already shown in the results. The variability of the bearing capacity for fine-grained soils can hence be significant. With regard to sand, cohesion values have a smaller influence, as they are generally small. The friction angle is hence of larger importance. As the friction angle is determined using CPT-test data, there is a small variability in the friction angle value and therefore as well in the bearing capacities.

Regarding deformations, the results show consistency. Soils with a high cone resistance, often sands, are the soils that deform the least. These soils are generally known as relatively stiff soils. On the contrary, soils with lower cone resistance, clay and especially peat, deform more compared to sand. This can be concluded from the results.

Comparing the results to real-life behaviour, the results comply with the values of the domains as shown in Figure 5, which means that the calculated deformations approximate real values. However, the model tends to predict relatively large deformations, considering the domains. This can possibly be explained by the fact that the Winkler model is a simplified model. Some real conditions of railway tracks are not included in the model (Sadeghi & Barati, 2010).

The parameters with the largest influence on the outcome of the deformation assessment are the cone resistance and the sleeve friction. As these parameters are the soil dependent parameters and they are determined using CPT-test data, the variability of these parameters and therefore the deformations is limited.

The extent to which the described model provides results that relate to real-life conditions is shown by combining the model with other models. According to El Laham (2021), the results for the Utrecht-Den Bosch trajectory have a predictive value regarding the condition of this trajectory. El Laham has created a model which relates structural information about a track structure to real-time measurements of the track structure and aims to make a predictor based on these relations. When the results from this research are included in El Laham’s model, the parameters strength and deformation are the two parameters that are the most decisive in predicting track failure. Accordingly, this research can contribute to the prediction of track condition and failure.

7. Conclusion

This research has aimed to answer the research question: *“What is the quantitative influence of soil on the track condition for the railway tracks between Utrecht and Den Bosch?”*

The influence of a soil is best described by the two most important failure types for railway tracks on a soil: progressive shear failure and excessive plastic deformation. These failure types are related to specific characteristics: strength and deformation.

A method to assess these characteristics is evaluated. The bearing capacity of a soil is used to assess the strength of a soil. Elastic deformations calculated from a beam-on-an-elastic-foundation model are used to assess the long-term behaviour of a soil related to deformations. The quality regarding both characteristics is evaluated for both passenger and cargo trains.

The trajectory Utrecht-Den Bosch is used to illustrate the evaluated method. The soil types along the trajectory are determined with a soil map and soil-dependent parameters are determined using available Cone Penetration Tests.

From this research can be concluded that a soil can have a significant influence on track condition. For the trajectory Utrecht-Den Bosch, the condition of the soil is good or moderate regarding repeated loading by passenger trains. This is the case for both the strength and the deformation assessment. The quality of the trajectory will not deteriorate by a large amount, though some deterioration on the long-term due to the soil cannot be excluded.

Considering cargo trains, the condition related to deformations is predominantly moderate, with a small number of sections of low quality. Limited deterioration on the long term can be expected, except for the parts with low quality, which will expectedly deteriorate quickly. Regarding strength, there is some variation due to the variable cohesion of soils. For lower bound cohesion values, the majority of the trajectory has a very low quality, whilst for upper bound values the quality of the trajectory is good or close to good. Since no specific value is found for the strength, the low quality sections will either deteriorate quickly or by a limited amount. The other sections will either deteriorate by a limited amount or not deteriorate at all.

8. Discussion

In this research, soil maps and data provided by CPT-tests have been used to determine the soil specific properties. All values have been derived directly from a map or test, have been interpolated or have been adjusted to other tests. Hence, if this research would be repeated, similar results will be acquired.

There are some limitations to the research that should be noted. This research has been done using available data. Several locations, however, have no data available, which requires the need for interpolation. As the distance between two measurements for some locations is substantial, the soil conditions and consequently the quality of these regions can be different from the values determined in this research. Another important factor to take into account is that the location from where the layer height of the top soil is determined and the location of a test do not always align. This can lead to a different estimation of the soil properties derived from tests. The availability of more tests and ground models can improve the reliability of the model.

Suggestions for future research are to investigate the influence of the soil under railway bridges and similar structures, which are not directly supported by the soil and to assess the condition of the combined track and soil under these structures. In combination with this research, this would enable a quality assessment on a complete trajectory. Another aspect after which more research can be done is the approach for determining missing values. Research can be done into the accuracy of the used interpolation method and into the applicability of other methods to estimate missing values.

References

ACS Distance Education. (2021). *Atmospheric Pressure*. Retrieved from https://www.acs.edu.au/info/sciences/physical-sciences/what-is-atmospheric-pressure.aspxe

Arthur, P. B., & Richard, J. S. (2002). Advanced mechanics of materials 6th. In *Advanced Mechanics of Materials*. John Wiley & Sons, inc.

Bathurst, J., Cai, Z. & Raymond, G. P. (1994). Estimate of Static Track Modulus Using Elastic Foundation Models. *Transportation Research Record, 1470, 6*, 65–72.

COB. (1997). *Gegevens Bovenbouw en Ballastbed* (JF/VC/70930 Vol.01). Holland Railconsult. Retrieved from https://www.cob.nl/wp-content/uploads/2018/01/L40011.pdf

Drenth, M. (2019, June 18). *Analyse TEN-T-specificaties voor Kernnetwerk Goederen*. Retrieved from https://www.rijksoverheid.nl/documenten/rapporten/2019/11/13/01-rapport-prorail-ten-t-specificaties-en-740m

El Laham, K. (2021). *Predicting Track Quality Using Structural Elements and Relative Track Geometry Data Measured by RILA: A Machine Learning Classification Approach*. [Unpublished Master Thesis]. Delft University of Technology.

Esveld, C. (2001). *Modern Railway Track* (Vol. 2). MRT-Productions.

Ibrahim, A., Huat, B. B. K., Asadi, A., & Nahazanan, H. (2014). Foundation and embankment construction in peat: An overview. *Electronic Journal of Geotechnical Engineering*, *19*(Z2), 10079–10094.

Li, D., & Selig, E. T. (1994). Track modulus: Its Meaning and Factors Influencing It. *Transportation Research Record, 1470, 1, 47-54*.

Li, D., & Selig, E. T. (1995). Evaluation of railway subgrade problems. *Transportation Research Record*, *1489*, 17–25.

Li, D., & Selig, E. T. (1998). Method for railroad track foundation design. *Journal of Geotechnical and Geoenvironmental Engineering, 124*(April), 316–322. https://doi.org/10.1061/(ASCE)1090-0241(1998)124:4(316)

McHenry, M. T., & Rose, J. G. (2012). *Railroad Subgrade Support and Performance Indicators — A Review of Available Laboratory and In-Situ Testing Methods*. Retrieved from http://trid.trb.org/view.aspx?id=1138428

Mosayebi, S., Esmaeili, M. & Zakeri, J. (2016). *Some Aspects of Support Stiffness Effects on Dynamic Ballasted Railway Tracks*. *60*(3). https://doi.org/10.3311/PPci.7933

Mosayebi, S., Esmaeili, M., & Zakeri, J. (2020). *Dynamic Train – Track Interactions and Stress Distribution Patterns in Ballasted Track Layers*. *146*(1). https://doi.org/10.1061/JPEODX.0000140

Nederlands Normalisatie-instituut. (2017). *Geotechnisch ontwerp van constructies – Deel 1: Algemene regels* (NEN 9997-1 +C2:2017). Retrieved from https://www.nen.nl/nen-9997-1-c2-2017-nl-240356

Nuevvo. (2021a). *Bearing capacity*. Retrieved from http://www.geotechdata.info/parameter/bearing-capacity

Nuevvo. (2021b). A*ngle of friction*. Retrieved from http://www.geotechdata.info/parameter/angle-of-friction

Nuevvo. (2021c). *Cohesion*. Retrieved from http://www.geotechdata.info/parameter/cohesion

Prakoso, P. B. (2016). The basic concepts of modelling railway track systems using conventional and finite element methods. *Info-Teknik*, *13*(1), 57–65.

ProRail. (2020). *Netverklaring 2020* (Vol. 2020, Issue december). Retrieved from https://www.prorail.nl/siteassets/homepage/samenwerken/vervoerders/documenten/2020-netverklaring-initieel.pdf

Rahman, M. H. (2018). Evaluation of Synthetic CPT and Soil Boring Data by Various Spatial Interpolation Techniques. *LSU Master's Thesis*. 4808. Retrieved from https://digitalcommons.lsu.edu/gradschool_theses/4808

Railplaza.nl. (2021). *Belastingen op het spoor*. Retrieved from https://www.railplaza.nl/belastingen-op-het-spoor/

Ramadan, M. I., Butt, S. D., & Popescu, R. (2015). *Effect of Padeye Depth on the Behavior of Offshore Anchor Piles Under Mooring Forces*. *June*. https://doi.org/10.1115/omae2015-41735

Rocscience Inc. (2016). *CPT Data Interpretation Theory Manual*. *1*, 18. Retrieved from https://www.rocscience.com/help/settle/pdf_files/theory/CPT_Theory_Manual.pdf

Sadeghi, J., & Barati, P. (2010). Improvements of conventional methods in railway track analysis and design. *Canadian Journal of Civil Engineering*, *37*(5), 675–683. https://doi.org/10.1139/L10-010

Saftner, D. (2018). Cone Penetration Test Design Guide for State Geotechnical Engineers. *Minnesota Department of Transportation*, *November*, 225. Minnesota Department of Transportation.

Sattler, P., Fredlund, D. G., Klassen, M. J., & Rowan, W. G. (1989). Bearing capacity approach to railway design using subgrade matric suction. *Transportation Research Record*, *1241*, 27–33.

Shahu, J. T., Kameswara Rao, N. S. V., & Yudhbir. (1999). Parametric study of resilient response of tracks with a sub-ballast layer. *Canadian Geotechnical Journal*, *36*(6), 1137–1150. https://doi.org/10.1139/t99-054

Stichting voor Bodemkartering. (1991). *Bodemkaart van Nederland - Algemene begrippen en indelingen*. Retrieved from http://maps.bodemdata.nl/pdf/ALGEMENE_BEGRIPPEN.pdf

Sun, Q. D., Indraratna, B., & Nimbalkar, S. (2016). Deformation and Degradation Mechanisms of Railway Ballast under High Frequency Cyclic Loading. *Journal of Geotechnical and Geoenvironmental Engineering*, *142*(1), 04015056. https://doi.org/10.1061/(asce)gt.1943-5606.0001375

Taylor & Francis Group, LLC. (2006). *Handbook of Railway Vehicle Dynamics*. CRC Press.

Ten Cate, J. A. M., Van Holst, A. F., Kleijer, H. & Stolp, J. (1995). *Handleiding bodemgeografisch onderzoek*. DLO-Staring Centrum. Retrieved from https://edepot.wur.nl/380626

TNO Geologische Dienst Nederland. (n.d.). *Ondergrondgegevens | DINOloket*. Retrieved June 1, 2021, from https://www.dinoloket.nl/ondergrondgegevens

TU Delft Library. (n.d.). *Bodemkaart van Nederland 1:50.000* [Map]. Retrieved April 21, 2021, from https://www.tudelft.nl/library/collecties/kaartenkamer/kaartencollectie/thematische-kaarten/bodemkaart-van-nederland-150000/

van Belkom, A. (2020). A simplified method for calculating load distribution and rail deflections in track, incorporating the influence of sleeper stiffness. *Advances in Structural Engineering*, *23*(11), 2358–2372. https://doi.org/10.1177/1369433220911144

Verruijt, A. (2010). *Grondmechanica*. Delft University of Technology. Retrieved from http://geo.verruijt.net/

Wang, H., Zeng, L., Bian, X., & Hong, Z. (2020). *Train Moving Load-Induced Vertical Superimposed Stress at Ballasted Railway Tracks*. *2020*. https:///doi.org/10.1155/2020/3428395

Appendix

Appendix A: Estimation of soil parameters

Various parameters are dependent on the soil type and admixture of a soil. If the soil type and admixture of a soil are known, Table A1 can be used to determine the parameters. The parameters that can be obtained from Table A1 are the friction angle *φ'*, the cohesion c', the dry volumetric weight γ_d and the saturated volumetric weight γ_s. The friction angle *φ'* for gravel and sand concerns lower bound values.

Table A1 Values for soil parameters based on soil type and admixture

Soil type	**Admixture**	***φ'* [deg] (a)**	***c'* [kPa] (2)**	**γ_d [kN/m^3] (3)**	**γ_s [kN/m^3] (3)**
Gravel		32	0	18	20
	Contains loam or clay	35	0	19	21
Sand		33	0	18	20
	Contains loam or clay	30	5	18	20
Loam	-	27,5	10 – 20	20	20
	Contains sand	27,5	10 – 20	19	19
Clay	-	17,5	10 – 20	17	17
	Contains sand	22,5	10 -- 20	18	18
Peat		15	-	10	10

(a) Gravel and sand values based on (1), values for other soils based on (3).

(1) Nuevvo, 2021b

(2) Nuevvo, 2021c

(3) Nederlands Normalisatie-instituut, 2017

Appendix B: Procedure for acquiring results

The results have been acquired using the method described in this research. Equations and evaluation approaches from previous chapters have been implemented in a spreadsheet to perform the calculations. The tables below show a sample of the spreadsheet.

As can be seen in Table B1, for each section with coordinates and length, the soil code from the soil map and the corresponding soil type and admixture have been listed. If a section is not included in the assessment, the reason why is listed in the column 'Not included'. Then, the soil properties to be acquired from CPT-tests are listed.

Table B1 Sample table of evaluation procedure: Part 1

X_Mid-point	**Y_Mid-point**	**Section length [m]**	**Not included**	**Soil code**	**Soil type**	**Ad-mixture**	q_c **[MPa]**	f_s **[MPa]**	σ_{v0} **[MPa]**	σ'_{v0} **[MPa]**
138134	453430	51,75		Rn67C	Clay	Sandy	7	0,03	0,007	0,007
138145	453357	200		Rn67C	Clay	Sandy	5,5	0,03	0,007	0,007
138194	453320	200		Rn67C	Clay	Sandy	1	0,03	0,007	0,007
138208	453245	56,25		Ro40C	Clay	-	2	0,01	0,007	0,007
138272	453175	128,5		Ro40C	Clay	-	2	0,01	0,007	0,007
138272	453134	200		Ro40C	Clay	-	2	0,01	0,007	0,007
138352	453032	200		Rn95A	Clay	Sandy	1,5	0,025	0,007	0,007
138376	452963	200		Rn95A	Clay	Sandy	1,5	0,025	0,007	0,007
138455	452860	200		Rn95A	Clay	Sandy	1	0,04	0,007	0,007
138479	452791	200		Rn95A	Clay	Sandy	1	0,04	0,007	0,007
138558	452689	200		Rn95C	Clay	Sandy	4	0,04	0,007	0,007
138581	452619	200		Rn95A	Clay	Sandy	4	0,04	0,007	0,007
138661	452518	200		Rn95C	Clay	Sandy	4	0,04	0,007	0,007
138684	452448	200		Rn95C	Clay	Sandy	4	0,04	0,007	0,007
138765	452347	200		Rn95C	Clay	Sandy	4	0,04	0,007	0,007
138788	452277	200		Rn95C	Clay	Sandy	4	0,04	0,007	0,007
138868	452175	200		Rn95C	Clay	Sandy	4	0,04	0,007	0,007
138891	452105	200		Rn95C	Clay	Sandy	4	0,04	0,007	0,007
138961	451998	200		Rn67C	Clay	Sandy	4	0,04	0,007	0,007
138976	451924	200		Rd10C	Sand	Clayey	8	0,03	0,007	0,007
139039	451814	200		Rd10C	Sand	Clayey	8	0,03	0,007	0,007
139052	451739	200		Rd10C	Sand	Clayey	8	0,03	0,007	0,007
139114	451629	200		Rd10C	Sand	Clayey	8	0,03	0,007	0,007
139127	451554	200		Rd10C	Sand	Clayey	8	0,03	0,007	0,007
139190	451444	200		Rd10C	Sand	Clayey	8	0,03	0,007	0,007
139203	451369	200		Rd10C	Sand	Clayey	8	0,03	0,007	0,007

Table B2 shows the next part of the spreadsheet. The soil parameters are determined using the approach as described in section 5.3. Q_{tn} and n are only applicable for sands and are therefore not evaluated for every section. For the cohesion, the lower bound value is listed. The calculations with the upper bound value for the cohesion, as listed in Table A1, have been done with the same spreadsheet. The column 'Dry or saturated' indicates whether dry or saturated conditions should be assumed.

Table B2 Sample table of evaluation procedure: Part 2

I_c	k_{sub}	Q_{tn}	n	φ' [deg]	c' lower bound	Dry or saturated	γ_d [kN/m³]	γ_s [kN/m³]
0,974	17,229			22,5	10	Sat.		18
1,068	15,126			22,5	10	Sat.		18
2,151	10,871			22,5	10	Sat.		18
1,371	8,118			17,5	10	Sat.		17
1,371	8,118			17,5	10	Sat.		17
1,371	8,118			17,5	10	Sat.		17
1,840	11,024			22,5	10	Sat.		18
1,840	11,024			22,5	10	Sat.		18
2,251	12,339			22,5	10	Sat.		18
2,251	12,339			22,5	10	Sat.		18
1,414	17,186			22,5	10	Sat.		18
1,414	17,186			22,5	10	Sat.		18
1,414	17,186			22,5	10	Sat.		18
1,414	17,186			22,5	10	Sat.		18
1,414	17,186			22,5	10	Sat.		18
1,414	17,186			22,5	10	Sat.		18
1,414	17,186			22,5	10	Sat.		18
1,414	17,186			22,5	10	Sat.		18
1,414	17,186			22,5	10	Sat.		18
0,895	17,828	132,66	0,19	40,95	5	Sat.		20
0,895	17,828	132,66	0,19	40,95	5	Sat.		20
0,895	17,828	132,66	0,19	40,95	5	Sat.		20
0,895	17,828	132,66	0,19	40,95	5	Sat.		20
0,895	17,828	132,66	0,19	40,95	5	Sat.		20
0,895	17,828	132,66	0,19	40,95	5	Sat.		20
0,895	17,828	132,66	0,19	40,95	5	Sat.		20

Table B3 shows the last part of the spreadsheet. The equations as described in chapter 4 are used to calculate the BCF and deformation for both cargo trains and passenger trains.

Table B3 Sample table of evaluation procedure: Part 3

Nq	**Nc**	**Nγ**	**q_u [kPa]**	**BCF Cargo**	**BCF Passenger**	**k_{total} [kN/m^2]**	**β**	**Deformation Cargo [mm]**	**Deformation Passenger [mm]**
8,23	17,45	5,99	195,4	1,53	1,79	7,980	0,0008	7,46	6,29
8,23	17,45	5,99	195,4	1,53	1,79	7,497	0,0008	7,81	6,59
8,23	17,45	5,99	195,4	1,53	1,79	6,279	0,0008	8,93	7,53
5,01	12,71	2,53	134,8	1,05	1,24	5,251	0,0007	10,21	8,61
5,01	12,71	2,53	134,8	1,05	1,24	5,251	0,0007	10,21	8,61
5,01	12,71	2,53	134,8	1,05	1,24	5,251	0,0007	10,21	8,61
8,23	17,45	5,99	195,4	1,53	1,79	6,329	0,0008	8,87	7,48
8,23	17,45	5,99	195,4	1,53	1,79	6,329	0,0008	8,87	7,48
8,23	17,45	5,99	195,4	1,53	1,79	6,742	0,0008	8,46	7,14
8,23	17,45	5,99	195,4	1,53	1,79	6,742	0,0008	8,46	7,14
8,23	17,45	5,99	195,4	1,53	1,79	7,970	0,0008	7,46	6,29
8,23	17,45	5,99	195,4	1,53	1,79	7,970	0,0008	7,46	6,29
8,23	17,45	5,99	195,4	1,53	1,79	7,970	0,0008	7,46	6,29
8,23	17,45	5,99	195,4	1,53	1,79	7,970	0,0008	7,46	6,29
8,23	17,45	5,99	195,4	1,53	1,79	7,970	0,0008	7,46	6,29
8,23	17,45	5,99	195,4	1,53	1,79	7,970	0,0008	7,46	6,29
8,23	17,45	5,99	195,4	1,53	1,79	7,970	0,0008	7,46	6,29
8,23	17,45	5,99	195,4	1,53	1,79	7,970	0,0008	7,46	6,29
8,23	17,45	5,99	195,4	1,53	1,79	7,970	0,0008	7,46	6,29
73,37	83,40	125,60	963,4	7,53	8,84	8,106	0,0008	7,37	6,21
73,37	83,40	125,60	963,4	7,53	8,84	8,106	0,0008	7,37	6,21
73,37	83,40	125,60	963,4	7,53	8,84	8,106	0,0008	7,37	6,21
73,37	83,40	125,60	963,4	7,53	8,84	8,106	0,0008	7,37	6,21
73,37	83,40	125,60	963,4	7,53	8,84	8,106	0,0008	7,37	6,21
73,37	83,40	125,60	963,4	7,53	8,84	8,106	0,0008	7,37	6,21
73,37	83,40	125,60	963,4	7,53	8,84	8,106	0,0008	7,37	6,21